Dynamics and Thermodynamics of the Low-Temperature Strongly Interacting Bose Gas

Nir Navon,[1,*] Swann Piatecki,[2,†] Kenneth Günter,[1] Benno Rem,[1] Trong Canh Nguyen,[1] Frédéric Chevy,[1] Werner Krauth,[2] and Christophe Salomon[1]

[1]*Laboratoire Kastler Brossel, CNRS, UPMC, École Normale Supérieure, 24 rue Lhomond, 75005 Paris, France*

[2]*Laboratoire de Physique Statistique, École Normale Supérieure, UPMC, Université Paris Diderot, CNRS, 24 rue Lhomond, 75005 Paris, France*

(Received 15 March 2011; revised manuscript received 21 June 2011; published 19 September 2011)

We measure the zero-temperature equation of state of a homogeneous Bose gas of ^{7}Li atoms by analyzing the *in situ* density distributions of trapped samples. For increasing repulsive interactions our data show a clear departure from mean-field theory and provide a quantitative test of the many-body corrections first predicted in 1957 by Lee, Huang, and Yang [Phys. Rev. **106**, 1135 (1957).]. We further probe the dynamic response of the Bose gas to a varying interaction strength and compare it to simple theoretical models. We deduce a lower bound for the value of the universal constant $\xi > 0.44(8)$ that would characterize the universal Bose gas at the unitary limit.

DOI: 10.1103/PhysRevLett.107.135301 PACS numbers: 67.85.−d, 05.30.Jp, 32.30.Bv, 67.60.Fp

From sandpiles to neuronal networks, electrons in metals, and quantum liquids, one of the greatest challenges in modern physics is to understand the behavior of strongly interacting systems. A paradigmatic example is superfluid ^{4}He, the understanding of which has resisted theoretical analysis for decades. Early attempts to address the problem of the strongly interacting Bose liquid focused on the dilute limit. A seminal result for the thermodynamics of the dilute Bose gas was the expansion of the ground state energy (per volume V), first obtained in the late 1950s [1]:

$$\frac{E}{V} = \frac{gn^2}{2}\left(1 + \frac{128}{15\sqrt{\pi}}\sqrt{na^3} + \cdots\right), \tag{1}$$

where n is the density of the gas, $g = 4\pi\hbar^2 a/m$ is the coupling constant for particles with mass m, and a is the s-wave scattering length, which characterizes the low-energy interactions. The first term in Eq. (1) is the mean-field energy, while the Lee-Huang-Yang (LHY) correction, proportional to $\sqrt{na^3}$, is due to quantum fluctuations [1]. Up to this order, the expansion is *universal*, in the sense that it depends solely on the gas parameter na^3 and not on microscopic details of the interaction potential [2–4].

Despite its fundamental importance, this expansion was never checked experimentally before the advent of ultracold quantum gases, where it became possible to tune the value of the scattering length using magnetic Feshbach resonances [5,6]. A first check of the LHY prediction was provided by recent experiments on strongly correlated Fermi gases [7–9] that behave as a gas of tightly bound dimers in the limit of small and positive values of a [10–12]. By contrast, early studies of Bose gases in the strongly interacting regime were plagued by severe inelastic atom loss [13], but recent experiments at JILA and Rice have revived interest in these systems and showed the onset of beyond mean-field effects [14,15]. Here we report on a quantitative measurement of the thermodynamic equation of state (EOS) of a strongly interacting atomic Bose gas in the low-temperature limit. We show that the EOS follows the expansion (1), and the comparison with fermionic systems illustrates the universality of the LHY correction.

In the first part, we restrict ourselves to a moderately interacting gas with negligible 3-body atom loss: $a/a_0 \sim 2000$, a_0 being the Bohr radius. In this regime our EOS reveals the Lee-Huang-Yang correction due to quantum fluctuations. We perform quantum Monte Carlo (QMC) simulations to support our zero-temperature approximation. We then test our assumption of thermal equilibrium by dynamically bringing the gas into a more strongly interacting regime where atom loss is no longer negligible. Finally, we explore the unitary regime where the scattering length is infinite.

Our experimental setup was described in [16]. Starting from a ^{7}Li cloud in a magneto-optical trap, we optically pump the atoms into the $|F = 2, m_F = 2\rangle$ hyperfine state and transfer them into a magnetic Ioffe trap. After evaporative cooling to a temperature of ~ 4 μK, the atoms are loaded into a hybrid magnetic/optical trap and then transferred to the $|F = 1, m_F = 1\rangle$ state. The radial optical confinement of the trap is provided by a single laser beam of 35 μm waist operating at a wavelength of 1073 nm, while the weak axial confinement is enhanced by an additional magnetic-field curvature. We apply a homogeneous magnetic field to tune the interaction strength by means of a wide Feshbach resonance that we locate at 737.8(2) G. The final stage of evaporation in the optical trap is carried out at a bias field of 717 G, where the scattering length has a value of about $200a_0$, and results in a Bose-Einstein condensate of $\sim 6 \times 10^4$ atoms with no discernible thermal part. In the final configuration the trapping frequencies are given by $\omega_r = 2\pi \times 345(20)$ Hz in the radial and $\omega_z = 2\pi \times 18.5(1)$ Hz in the axial direction. The magnetic bias field is then adiabatically ramped

to the vicinity of the Feshbach resonance in 150 ms and the density distribution is recorded using *in situ* absorption imaging (Fig. 1). As the EOS critically depends on the scattering length, a precise knowledge of the latter close to the Feshbach resonance is essential. In view of the discrepancy between two recent works [15,17], we have independently calibrated the scattering length $a(B)$ as a function of magnetic field B by radio-frequency molecule association spectroscopy [18], as described in the Supplemental Material [19].

For the measurement of the EOS, we follow the method of [9,20–23]. Accordingly, the local pressure $P(z)$ along the symmetry axis of a harmonically trapped gas is related to the doubly integrated *in situ* density profile $\bar{n}(z) = \int dxdyn(x, y, z)$:

$$P(\mu_z) = \frac{m\omega_r^2}{2\pi}\bar{n}(z). \tag{2}$$

This formula relies on the local-density approximation in which the local chemical potential is defined as $\mu_z = \mu_0 - \frac{1}{2}m\omega_z^2 z^2$, where μ_0 is the global chemical potential of the gas.

To measure the pressure at different interaction strengths we have selected images with atom numbers in the range of 3–4 $\times 10^4$ in order to avoid high optical densities during absorption imaging while keeping a good signal-to-noise ratio. A total of 50 images are used, spanning values of a/a_0 from 700 to 2150. We calibrate the relation between the integrated optical density and the pressure of the gas at weak interaction, well described by mean-field theory (inset of Fig. 2). The density profiles then generate the EOS (2). The global chemical potential μ_0 remains to be determined. For this work, we infer μ_0 self-consistently in a model-independent way from the density profiles (see the Supplemental Material [19]).

In the dilute limit $na^3 \ll 1$, where the EOS is universal, dimensional analysis can be used to write the grand canonical EOS of the homogeneous Bose gas at zero temperature in the form

$$P(\mu, a) = \frac{\hbar^2}{ma^5}h(\nu), \tag{3}$$

where $\nu \equiv \mu a^3/g$ is the (grand canonical) gas parameter and $h(\nu)$ is the normalized pressure. This EOS contains all thermodynamic macroscopic properties of the system. For example, the energy can be deduced from the pressure using a Legendre transform detailed in the Supplemental Material [19], and in particular, its LHY asymptotic expansion (1). According to the above definition of h, the mean-field EOS simply reads $h(\nu) = 2\pi\nu^2$. These predictions for $h(\nu)$ are compared to the experimental data points in Fig. 2, and to our QMC calculation. We observe a clear departure of the EOS from the mean-field prediction [dashed gray line (dashed red online)]. At the largest measured value of $\nu = 2.8 \times 10^{-3}$ our data show a reduction of 20% of the pressure with respect to the mean-field result.

We observe that LHY theory accurately describes our experimental data and is hardly distinguishable from the

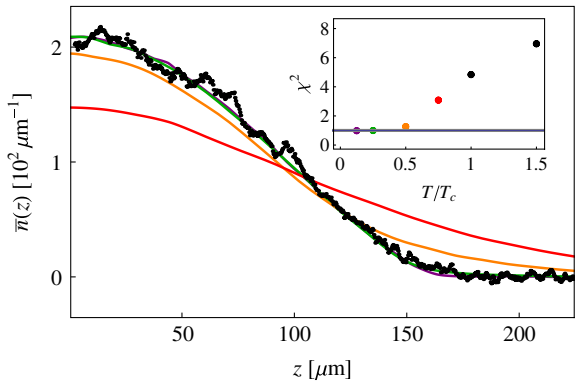

FIG. 1 (color online). Doubly integrated density profile of a trapped Bose gas at a scattering length $a/a_0 = 2150$, used to measure the LHY expansion (1). The average over 5 experimental images is shown in black points. The QMC predictions for 3.9×10^4 atoms are plotted in a solid line for $T/T_c = 0.75$ in red, 0.5 in orange, 0.25 in green, and 0.125 in purple (solid lines from bottom to top). Inset: χ^2 deviation per degree of freedom of a single experimental density profile with QMC results at different temperatures. The excellent agreement between experimental profiles and QMC validates the zero-temperature assumption for the EOS measurement.

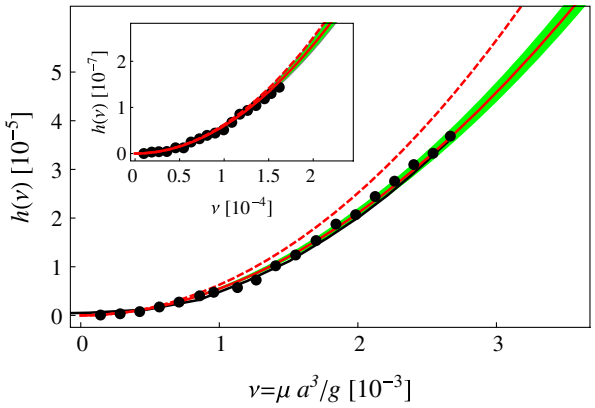

FIG. 2 (color online). Equation of state of the homogeneous Bose gas expressed as the normalized pressure h as a function of the gas parameter ν. The gas samples for the data shown in the main panel (inset) have been prepared at scattering lengths of $a/a_0 = 1450$ and 2150 ($a/a_0 = 700$). The gray (red online) solid line corresponds to the LHY prediction, and the gray (red online) dashed line to the mean-field EOS $h(\nu) = 2\pi\nu^2$. In the weakly interacting regime the data are well described by mean-field theory (inset), in opposition to stronger interactions where beyond-mean-field effects are important (main panel). The QMC EOS at $T/T_c = 0.25$ (solid black line) is nearly indistinguishable from the LHY EOS. The shaded (green online) area delimits the uncertainty of 5% on the value of a.

QMC in the studied range of interaction strength, a point already put forward in a diffusion Monte Carlo simulation at even higher values of the gas parameter [24]. We can quantify the deviation of our data from mean-field theory by fitting the measured EOS with a function that includes a correction of order $\sqrt{na^3}$. For this purpose we convert the energy $E/N = [2\pi\hbar^2/(ma^2)]na^3[1 + \alpha(na^3)^{1/2}]$ to the grand canonical EOS (see the Supplemental Material [19]) and use α as a fit parameter in the resulting pressure $P(\mu)$. The fit yields the value $\alpha = 4.5(7)$, which is in excellent agreement with the theoretical result $128/(15\sqrt{\pi}) \approx 4.81$ in Eq. (1). Together with the measurement with composite bosons of [9], this provides a striking check of the universality predicted by the expansion (1) up to order $\sqrt{na^3}$ [11].

In the above interpretation we assumed that the zero-temperature regime has effectively been reached. To check this crucial assumption, we have performed finite-temperature path-integral quantum Monte Carlo simulations [25] in the anisotropic harmonic trap geometry of the experiment with continuous space variables. The experimental atom number can be reached without difficulty and pair interactions are described by a pseudopotential. All thermodynamic properties of the gas at finite temperature are obtained to high precision and without systematic errors. As seen in Fig. 1, we find good agreement between the experimental density distributions and the QMC profiles at temperatures up to $0.25T_c$, where T_c is the condensation temperature of the ideal Bose gas. This shows that thermal effects are negligible and lead to an error in the EOS much smaller than the statistical error bars in Fig. 2.

We now assess the adiabaticity of the interaction sweep in the measurements described above. A violation of adiabaticity could lead to nonequilibrium density profiles that distort the measured EOS. We study the dynamics of the Bose gas subjected to time-dependent interaction sweeps into increasingly strongly interacting regimes, where the enhanced three-body loss rate limits the practical duration of the sweep. In Fig. 3 we plot the axial cloud size determined by a Thomas-Fermi fit as a function of the sweep duration. The magnetic field is ramped approximately linearly in time, sweeping a/a_0 from an initial value of 200 to different final values. Besides the experimental data we present theoretical results from a mean-field scaling solution [26,27] and from a solution of the hydrodynamic equations incorporating the LHY EOS based on a variational scaling ansatz [28]. The latter shows a remarkable agreement with our experimental data for $a \leq 3000a_0$. For scattering lengths $a/a_0 \leq 840$ the radius is nearly constant for sweep durations $\tau\omega_z/(2\pi) > 1.5$ ($\tau > 80$ ms), indicating that the cloud follows the interaction strength adiabatically. For the largest value used in the EOS study ($a/a_0 = 2150$), the atom loss is less than 4% and the cloud size after the $\tau = 150$ ms sweep [$\tau\omega_z/(2\pi) \gtrsim 2.8$] is 2.5%

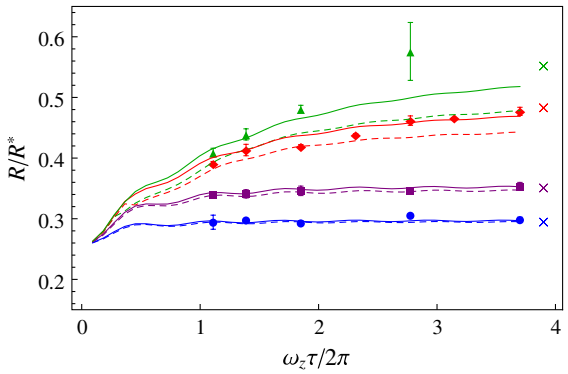

FIG. 3 (color online). Radius R of the Bose gas as a function of the duration τ of the interaction sweep. The radius R is normalized to the radius $R^* = a_{\rm ho}(15\lambda^2 N)^{1/5}$ [where $a_{\rm ho} = (\hbar/m\omega_z)^{1/2}$ and $\lambda = \omega_r/\omega_z$]. N is the measured atom number at the end of each sweep. The final values of a/a_0 are 380 (blue dots), 840 (purple squares), 2940 (red diamonds), and 4580 (green triangles). The solid (dashed) lines show the solution of a variational hydrodynamic approach (mean-field scaling solutions). The crosses show the predicted equilibrium beyond-mean-field radii.

smaller than the equilibrium value. We have corrected for this systematic effect by rescaling the measured density n_0 for the determination of the EOS, $\bar{n} = \eta^{-1}\bar{n}_0(\eta z)$ (with $\eta = 0.975$ for $a/a_0 = 2150$).

The properties of the Bose gas for very large values of na^3 constitute a challenging open problem. Because of the

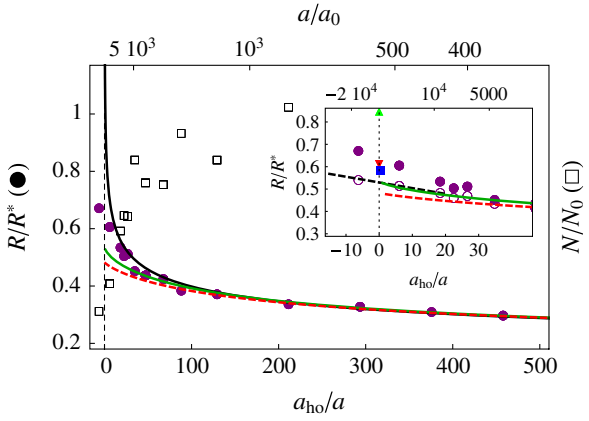

FIG. 4 (color online). Normalized cloud radius $R_{\rm TF}/R^*$ (filled purple circles) and normalized atom number (open black squares) as a function of the inverse scattering length $a_{\rm ho}/a$ at the end of a 75-ms magnetic-field sweep. The static mean-field prediction is plotted in a solid black line, the mean-field scaling solution in a dashed red line, and the beyond mean-field scaling ansatz in a solid gray line (green online). Inset: Zoom around the unitary limit. Predictions for the universal constant ξ are shown in an up triangle [34], down triangle [33], and square [32]. The filled (empty) circles correspond to the radii normalized to the final (initial) atom number (see [31]). The dashed black line is the linear interpolation at unitarity.

experimental limitation imposed by three-body recombination, we access this region with a shorter sweep of duration $\tau\omega_z/(2\pi) = 1.35$ ($\tau \approx 75$ ms). In Fig. 4 we plot the normalized radius of the Bose gas as a function of the inverse scattering length a_{ho}/a. Deep in the mean-field regime ($a \lesssim 800a_0$) the ramp is adiabatic as the data match the equilibrium Thomas-Fermi prediction. As the scattering length is increased, both nonadiabaticity and beyond mean-field effects become important. A departure from the equilibrium result becomes evident above a scattering length of $\simeq 2000a_0$. Taking into account the mean-field dynamics gives an improved description of our data (red dashed line). Even better agreement (up to values of $a/a_0 \simeq 5000$) is obtained with the variational approach incorporating the LHY correction as presented above [gray solid line (green online)] [28]. Probing larger values of the scattering length enables us to gain further insight into the unitary Bose gas, $a = \infty$. Because of the low densities of our samples, only half of the atoms are lost at the end of the sweep to the resonance (see squares in Fig. 4). Universal thermodynamics at unitarity have been conjectured for quantum gases [29] and successfully checked experimentally for Fermi gases [30]. In the case of bosonic atoms the existence of a many-body universal state at unitarity is still unknown. Under the assumption of universality, the only relevant length scale should be the interparticle spacing $n^{-1/3}$ and the EOS would take the form $\mu \propto \frac{\hbar^2}{m} n^{2/3}$. Up to a numerical factor, this EOS is identical to that of an ideal Fermi gas and we can write $\mu = \xi E_F$ [where $E_F = \hbar^2/2m(6\pi^2 n)^{2/3}$]. As we increase the scattering length towards the unitarity regime, the cloud is expected to grow in size. Because of the finite response time of the gas, it is reasonable to assume that the measured radius R is smaller than the equilibrium radius. From this inequality, in the spirit of variational methods, we deduce a lower bound for the value of ξ by interpolating our data at unitarity [black dashed line in the inset of Fig. 4]: $\xi > 0.44(8)$ [31]. This bound is satisfied for the predictions $\xi = 0.66$ [32] and for the upper bounds from variational calculations, 0.80 [33] and 2.93 [34].

Future work could focus on the measurement of the condensate fraction since the quantum depletion is expected to be as large as $\sim$8% for our most strongly interacting samples in equilibrium, and on finite-temperature thermodynamic properties [35]. Our measurements on resonance as well as future theoretical studies should give crucial insights on the unitary Bose gas.

We are grateful to Y. Castin, F. Werner, X. Leyronas, S. Stringari, S. Giorgini, S. Pilati, and A. Grier for discussions and to C. Lancien, I. Lahlou, S. El-Ghazzal, T. Vu, and L. Bernard for experimental assistance. We thank J. Dalibard and S. Nascimbène for useful comments on the manuscript. We acknowledge support from ESF Euroquam (FerMix), ANR FABIOLA, Région Ile de France (IFRAF), ERC, and Institut Universitaire de France.

*navon@ens.fr
†swann.piatecki@ens.fr

[1] T. D. Lee, Kerson Huang, and C. N. Yang, Phys. Rev. **106**, 1135 (1957).
[2] K. Brueckner and K. Sawada, Phys. Rev. **106**, 1117 (1957).
[3] S. Beliaev, JETP **7**, 289 (1958).
[4] E. Lieb, Phys. Rev. **130**, 2518 (1963).
[5] S. Inouye *et al.*, Nature (London) **392**, 151 (1998).
[6] J. Roberts *et al.*, Phys. Rev. Lett. **85**, 728 (2000).
[7] A. Altmeyer *et al.*, Phys. Rev. Lett. **98**, 40 401 (2007).
[8] Y. Shin *et al.*, Phys. Rev. Lett. **101**, 070404 (2008).
[9] N. Navon *et al.*, Science **328**, 729 (2010).
[10] G. Astrakharchik *et al.*, Phys. Rev. Lett. **93**, 200404 (2004).
[11] X. Leyronas and R. Combescot, Phys. Rev. Lett. **99**, 170402 (2007).
[12] H. Hu *et al.*, Europhys. Lett. **74**, 574 (2006).
[13] P. Fedichev *et al.*, Phys. Rev. Lett. **77**, 2921 (1996).
[14] S. Papp *et al.*, Phys. Rev. Lett. **101**, 135301 (2008).
[15] S. Pollack *et al.*, Phys. Rev. Lett. **102**, 90402 (2009).
[16] S. Nascimbene *et al.*, Phys. Rev. Lett. **103**, 170402 (2009).
[17] N. Gross *et al.*, Phys. Rev. Lett. **105**, 103203 (2010).
[18] J. Zirbel *et al.*, Phys. Rev. A **78**, 13 416 (2008).
[19] See Supplemental Material at http://link.aps.org/supplemental/10.1103/PhysRevLett.107.135301 for technical details about the density profiles analysis and Feshbach resonance calibration.
[20] C. H. Cheng and S. K. Yip, Phys. Rev. B **75**, 14 526 (2007).
[21] Y. I. Shin, Phys. Rev. A **77**, 41 603 (2008).
[22] T. Ho and Q. Zhou, Nature Phys. **6**, 131 (2009).
[23] S. Nascimbene *et al.*, Nature (London) **463**, 1057 (2010).
[24] S. Giorgini, J. Boronat, and J. Casulleras, Phys. Rev. A **60**, 5129 (1999).
[25] W. Krauth, Phys. Rev. Lett. **77**, 3695 (1996).
[26] Y. Castin and R. Dum, Phys. Rev. Lett. **77**, 5315 (1996).
[27] Y. Kagan, E. L. Surkov, and G. V. Shlyapnikov, Phys. Rev. Lett. **79**, 2604 (1997).
[28] The details of the time-dependent analysis will be published elsewhere.
[29] T. L. Ho, Phys. Rev. Lett. **92**, 90 402 (2004).
[30] M. Inguscio, W. Ketterle, and C. Salomon, *Proceedings of the International School of Physics Enrico Fermi, Course CLXIV* (IOS Press, Amsterdam, 2006).
[31] At unitarity, the cloud radius R would scale as $N^{1/6}\xi^{1/4}$. The normalization R^* used in Fig. 4 scales as $N^{1/5}$ so that $R/R^* \propto \xi^{1/4}N^{-1/30}$ very slowly depends on the atom number. In order to take into account the changing atom number near unitarity and obtain a safe experimental lower bound on $\xi \propto (R/R^*)^4 N^{2/15}$, we minimize both R/R^* and $N^{2/15}$. This is done by taking for R/R^* the initial atom number (empty circles in the inset of Fig. 4), and the final, for $N^{2/15}$.
[32] Y.-L. Lee and Y.-W. Lee, Phys. Rev. A **81**, 063613 (2010).
[33] J. L. Song and F. Zhou, Phys. Rev. Lett. **103**, 25302 (2009).
[34] S. Cowell *et al.*, Phys. Rev. Lett. **88**, 210403 (2002).
[35] R. Smith, R. Campbell, N. Tammuz, and Z. Hadzibabic, Phys. Rev. Lett. **106**, 250403 (2011).